Journal of
Materials Chemistry A

Accepted Manuscript

This is an *Accepted Manuscript*, which has been through the RSC Publishing peer review process and has been accepted for publication.

Accepted Manuscripts are published online shortly after acceptance, which is prior to technical editing, formatting and proof reading. This free service from RSC Publishing allows authors to make their results available to the community, in citable form, before publication of the edited article. This *Accepted Manuscript* will be replaced by the edited and formatted *Advance Article* as soon as this is available.

To cite this manuscript please use its permanent Digital Object Identifier (DOI®), which is identical for all formats of publication.

More information about *Accepted Manuscripts* can be found in the **Information for Authors**.

Please note that technical editing may introduce minor changes to the text and/or graphics contained in the manuscript submitted by the author(s) which may alter content, and that the standard **Terms & Conditions** and the **ethical guidelines** that apply to the journal are still applicable. In no event shall the RSC be held responsible for any errors or omissions in these *Accepted Manuscript* manuscripts or any consequences arising from the use of any information contained in them.

Journal of Materials Chemistry A

Cite this: DOI: 10.1039/b000000x

www.rsc.org/xxxxxx

Communication

Enhancement of power conversion efficiency in a polymer solar cell using a work-function-controlled $Ti_mSi_nO_x$ interlayer

Soo-Ghang Ihn,*[a] Younhee Lim,[a] Sungyoung Yun,[a] Insun Park,[a] Jong Hwan Park,[a] Yeonji Chung,[a] Xavier Bulliard,[a] Jaejune Chang,[a] Hyeran Choi,[a] Jong Hyeok Park,[b] Yeong Suk Choi,*[a] Gyeong-Su Park[a] and Hyuk Chang[a]

Received (in XXX, XXX) Xth XXXXXXXXX 20XX, Accepted Xth XXXXXXXXX 20XX
DOI: 10.1039/b000000x

Work-function-adjustable $Ti_mSi_nO_x$ provides an opportunity to optimize the energy-level alignment at the photoactive/cathode interface in the polymer bulk heterojunction solar cell. The work function of $Ti_mSi_nO_x$ is engineered by adjusting the Si mol% during the sol-gel reaction. The controlled work function provides an energetically downhill cascade pathway for electrons from the electron acceptor to the cathode, which contributes to improvement in electron collection at the cathode. The valence band maxima of $Ti_mSi_nO_x$ also become deeper as the Si mol% increases and the hole-blocking ability of $Ti_mSi_nO_x$ is enhanced as a result. Accordingly, polymer solar cells fitted with the optimized $Ti_mSi_nO_x$ exhibit enhanced performance.

Introduction

Polymer solar cells (PSCs) have attracted considerable attention owing to their potential for the fabrication of low-cost, lightweight, mechanically flexible modules. However, their power conversion efficiency (PCE) needs to be improved if PSCs are to penetrate the solar energy market. For this to be achieved, a harmonic combination of donor polymer properties such as light absorption, charge transport, miscibility and energy-level alignment with a given acceptor is essential. Besides, the interfacial engineering between the photoactive layer and electrodes is also very important because the interlayers lead to selective charge collection at the electrodes when the bulk heterojunction (BHJ) is employed as a photoactive layer.[1-3] Because of the unique structure of BHJ, both the donor and acceptor domains can form contacts with both electrodes simultaneously. Therefore, the probability of recombination at both electrodes is so high that it may decrease the open circuit voltage (V_{oc}) and the fill factor (FF).[4] For recombination suppression, interlayers exhibiting asymmetric charge transport are usually inserted at the BHJ photoactive layer/electrode interfaces.[5-8] Asymmetric charge transport has usually been achieved through energy-level alignment between the photoactive material (donor or acceptor) and the interlayer. In particular, for electron-transport enhancement with simultaneous suppression of hole transport, TiO_x or ZnO layers has been utilized as a cathode interlayer because their work functions are quite similar to the lowest unoccupied molecular orbital (LUMO) of [6,6]-phenyl-C_{71}-butyric acid methyl ester ($PC_{71}BM$), while their valence band maxima (VBM) are much deeper than the highest occupied molecular orbital (HOMO) of typical donor materials.[5,6,9-14] The work function (of TiO_x or ZnO) must be similar to that of the LUMO of $PC_{71}BM$ for efficient electron collection. The "energetically downhill cascade pathway" for electrons from $PC_{71}BM$ to Al has been suggested to improve the electron-collection efficiency.[15-19] For tuning of the work function of a given interlayer for such fine energy-level alignment with $PC_{71}BM$, additional post-treatments have been tested and employed on the surface of TiO_x (or ZnO), such as oxygen plasma treatment,[20] UV-ozone treatment[21] and self-assembled monolayer deposition,[22-26] but these incur additional process costs. Furthermore, they hardly change the bandgap of TiO_x (or ZnO), so it is impossible to engineer the VBM of TiO_x (or ZnO) simultaneously, although a deep VBM of TiO_x (or ZnO) is required for more effective hole blocking in the BHJ solar cell.

In this work, we suggest a novel ternary oxide ($Ti_mSi_nO_x$, $m + n = 1$) sol-gel film as a cathode interlayer, which has a work function and bandgap that can be tuned simultaneously by adjusting its composition ratio (m/n) during the sol-gel reaction. The details of the $Ti_mSi_nO_x$ synthesis are provided in the Experimental section with a scheme. The work-function-, and bandgap-engineered $Ti_mSi_nO_x$ is tested in a PSC using one of the most promising donor polymers, poly[4,8-bis-substituted-benzo(1,2-*b*:4,5-*b'*)dithiophene-2,6-diyl-*alt*-4-substituted-thieno(3,4-*b*)thiophene-2,6-diyl] (PBDTTT)-derived polymer,[27-30] with $PC_{71}BM$. The chemical structure and absorption spectrum of the polymer (fluorinated PBDTTT functionalized with a compatibilizing ethoxycarbonyl butyl carboxyl group, PBDTTT-F-ECB) employed in this work are shown in Fig. 1 (a) and (b), respectively, together with those of $PC_{71}BM$. Details of PBDTTT-F-ECB will be presented elsewhere.

Experimental

Preparation of $Ti_mSi_nO_x$ sol-gel solutions

The solution for the formation of the $Ti_mSi_nO_x$ interlayer was prepared through sol-gel reaction, as illustrated in Scheme 1. A solution of tetraethyl orthosilicate (TEOS, 0.013 mol, 2.88 mL) and HCl (37 %, 0.13 mmol, 0.013 mL) in methanol (MeOH, 5.00 mL) was stirred at room temperature in a vial. Titanium (IV)

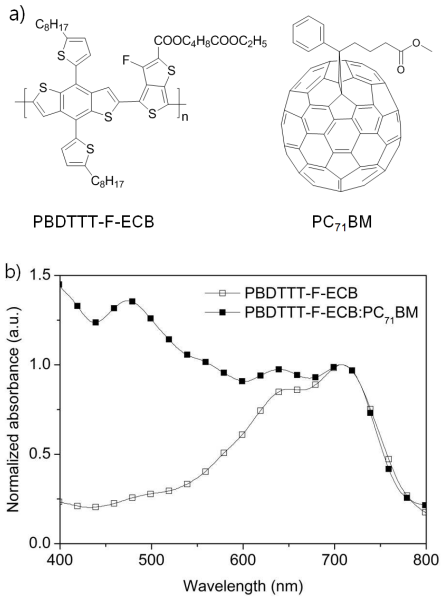

Fig. 1 a) Chemical structures of PBDTTT-F-ECB and $PC_{71}BM$. b) Absorption spectra of PBDTTT-F-ECB and its blend with $PC_{71}BM$.

isopropoxide (TIP, 0.013 mol, 4.08 mL) was added to MeOH (5.00 mL). Glacial acetic acid (0.013 mol, 0.761 mL) was then added dropwise at room temperature. After stirring for 30 min, the appropriate portion of TEOS solution was dropped into TIP solution for the target mole ratio of TEOS to TIP. The mixture was stirred at 60 °C for 6 h. Subsequently, the mixture was cooled down to room temperature and stirred for 18 h. The reaction mixture was stirred vigorously during the entire reaction. The solution was diluted in MeOH (1:400) before use.

Fabrication of polymer solar cells

Each cell was fabricated on a cleaned indium tin oxide (ITO)-coated glass substrate with the structure: glass/ITO/poly(3,4-ethylenedioxythiophene):poly(styrene) sulfonate (PEDOT:PSS)/ polymer:$PC_{71}BM$/$Ti_mSi_nO_x$/Al. Aqueous PEDOT:PSS solution (Baytron P VP A1 4083, used as purchased) was spin-cast to form a 30-nm film on the ITO glass substrate. The PEDOT:PSS-coated ITO/glass substrate was dried at 120 °C in an air-filled natural convection oven for 1 h and then transferred into a nitrogen-filled glove box. The blend solution containing the polymer (PBDTTT-F-ECB):$PC_{71}BM$ mixture in chlorobenzene with 4-vol% 1,8-diiodooctane was then spin-cast on the PEDOT:PSS layer. $PC_{71}BM$ (Sigma-Aldrich) was used as purchased. The active film was dried at room temperature for 30 min. The $Ti_mSi_nO_x$ sol-gel solution diluted in MeOH was then spin-cast on the active layer. The Al cathode electrode was deposited by thermal evaporation in vacuum with a base pressure of less than 9×10^{-7} torr, and was over 100 nm in thickness.

Measurement and characterization

The work function of $Ti_mSi_nO_x$ was measured using ultraviolet photoelectron spectroscopy (UPS) (PHI 5000 VersaProbe). The energy bandgap of $Ti_mSi_nO_x$ was obtained from the cutoff wavelength of its absorption spectrum. Total reflection spectra

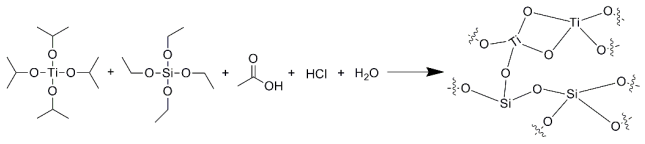

Scheme 1 Formation of $Ti_mSi_nO_x$ by sol-gel reaction.

were obtained with a UV-vis spectrometer (PerkinElmer, Lambda 35 with a 50-mm integrating sphere) after calibration with a barium reference. The total absorption (A) was obtained from the total reflection ($R = 1 - A$) including both direct and diffuse reflections measured in the integrating sphere with the inside wall coated with barium sulfate. The J-V characteristics of the devices were measured with a Keithley 2400 Source-Meter and Oriel xenon lamp with an air mass (AM) 1.5 filter under nitrogen gas in a glove box. The intensity of the simulated light (100 mW cm^{-2}) was calibrated with a KG-5 filtered standard Si cell. The active area was defined for obtaining J_{sc} using the measured area of the Al top electrode. The series and shunt resistance (R_s and R_p) were calculated from the inverse slope of the J-V curves at 0 and 1.5 V, respectively.[11,12] IPCE measurements of the devices without encapsulation were performed in air within minutes after the J-V measurements (Newport, Model IQE-200). Transmission electron microscopy (TEM) and energy-dispersive spectroscopy (EDS) were performed with FEI, Tecnai-G2 F20. TEM samples were prepared with a focused ion beam. The refractive index of $Ti_{0.5}Si_{0.5}O_x$ was determined by spectroscopic ellipsometry. (J. A. Woollam Co., Inc.)

Results and discussion

To find the best composition ratio of $Ti_mSi_nO_x$ for efficient electron collection and hole blocking at the cathode, we investigated the work function and bandgap of $Ti_mSi_nO_x$. The bandgap was estimated from the cutoff wavelength of the absorption spectrum (see ESI, Fig. S1).[31] VBM was calculated from the sum of the work function and the optical bandgap. Fig. 2 (a) shows that the work function of $Ti_mSi_nO_x$ increases with Si mol%. The required work function (between those of $PC_{71}BM$ and Al, i.e., 3.93 eV < Φ < 4.06 eV) to complete the downhill cascade pathway for electrons from $PC_{71}BM$ to Al is obtained at around 50 mol% Si ($Ti_{0.5}Si_{0.5}O_x$), as illustrated in the insert of Fig. 2 (a). The bandgap (E_g) of $Ti_mSi_nO_x$ increases slightly with Si mol% (Fig. 2 (b)); it becomes saturated at 10% and does not change much by 50%. The E_g value of $Ti_{0.5}Si_{0.5}O_x$ exhibiting the optimum work function is 3.82 eV. It is believed that the increased E_g and the work function of $Ti_{0.5}Si_{0.5}O_x$ would lead to a higher barrier against hole transport to the cathode. The strong hole-blocking ability of $Ti_{0.5}Si_{0.5}O_x$ is expected because of such a higher barrier and it is verified by measuring the leakage current of the device. Fig. 2 (c) shows the diode characteristics of the four PSCs with different cathodes: (i) none/Al; (ii) 1-nm LiF/Al; (iii) 20-nm Ca/Al; (iv) 4-nm $Ti_{0.5}Si_{0.5}O_x$/Al; (v) 4-nm TiO_x; and (vi) 4-nm SiO_x, without light exposure. The current density at -3 V of the PSC with $Ti_{0.5}Si_{0.5}O_x$, TiO_x or SiO_x is much lower than those of other PSCs, confirming the better hole-blocking ability of wide band gap sol-gel $Ti_mSi_nO_x$. SiOx looks better than other $Ti_mSi_nO_x$ although there are only small differences in leakage current. It is in good agreement with the deeper VBM of the

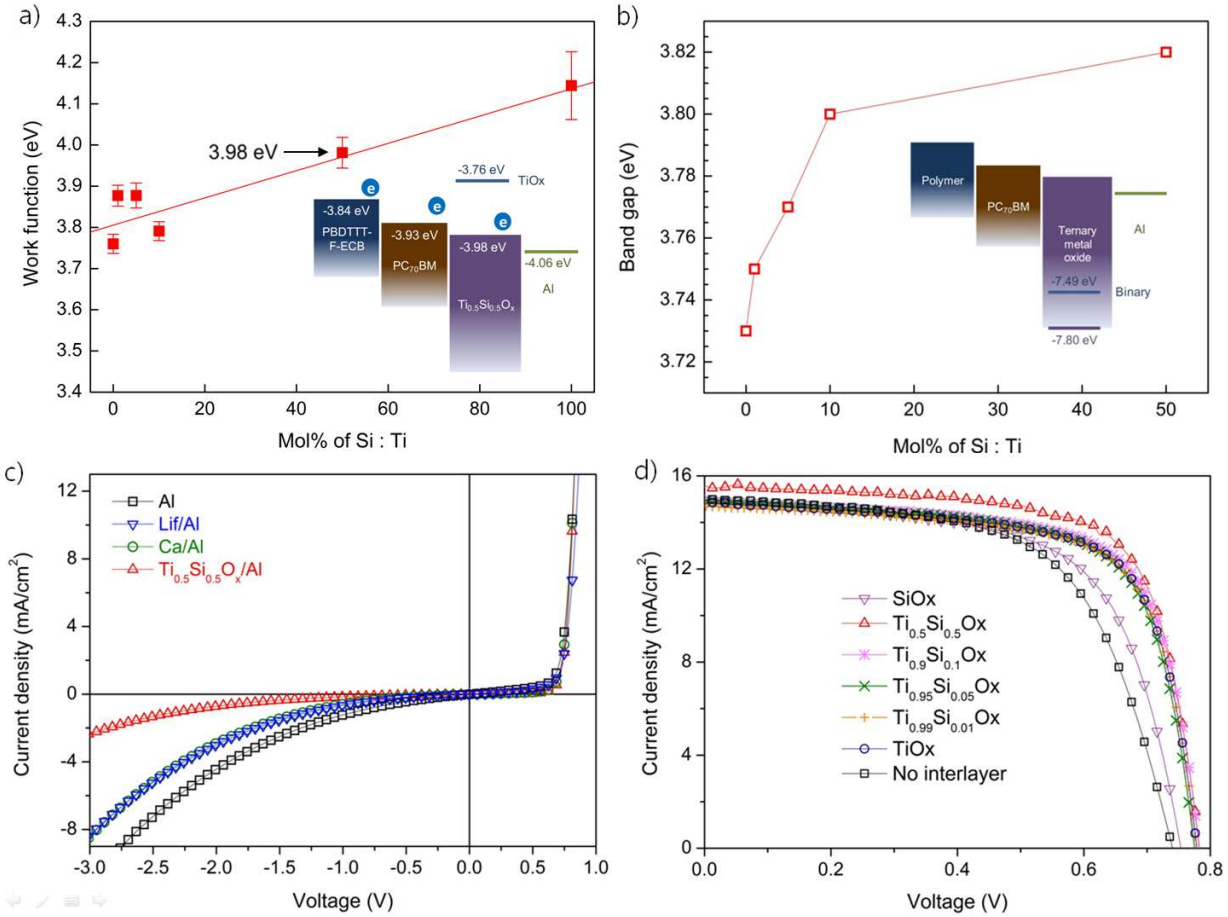

Fig. 2 a) Work function and b) energy bandgap of the $Ti_mSi_nO_x$ layer as functions of Si mole fraction. The insets are schematic diagrams showing tuned $Ti_{0.5}Si_{0.5}O_x$ forming an energetically downhill cascade pathway for electrons. c) Leakage current in reverse bias for the devices with the four different cathodes. d) *J-V* characteristics of the solar cells using $Ti_mSi_nO_x$ with various composition ratios ($m + n = 1$)

Table 1 Efficiency parameters of the devices employing various $Ti_mSi_nO_x$ interlayers with different compositions.

Si [%]	V_{oc} [mV]	J_{sc} [mA cm^{-2}]	FF [%]	PCE [%]		R_s	R_p
				Best	Ave.[a]	[Ω cm^2]	
0	778.0	14.9	69.1	8.01	7.80	1.6	1082
1	775.7	14.7	69.2	7.89	7.71	1.3	1106
5	773.5	14.9	70.1	8.08	7.87	1.1	1116
10	780.2	15.1	69.1	8.14	8.05	1.1	1163
50	782.4	15.6	70.8	8.64	8.53	1.1	1499
100	740.1	14.9	64.8	7.14	7.02	2.3	928
Al-only	735.9	14.9	61.3	6.72	6.54	4.0	858

[a] Average values were obtained from a minimum of 4 devices for each composition.

higher Si-content $Ti_mSi_nO_x$. The reason why the difference in leakage between the three oxides is small is probably that the VBM of the oxides are all deep enough already. Photovoltaic performance of the PBDTTT-F-ECB:$PC_{71}BM$ solar cell using $Ti_mSi_nO_x$ with various Si mol% values were also investigated. Fig. 2 (d) shows the *J-V* characteristics under illumination (1 sun) and the efficiency parameters are summarized in Table 1. The interlayer with 50-mol% Si exhibits the highest efficiency with low R_s and high R_p, which verify its high electron-collection efficiency and hole-blocking ability, respectively. The low Si mol% (0, 1, 5, 10%) $Ti_mSi_nO_x$ interlayers also give rise to a considerable enhancement of the photovoltaic performance, albeit less than that of $Ti_{0.5}Si_{0.5}O_x$. The PSC using the SiO_x (100 mol% Si) interlayer exhibits improved V_{oc} and FF values compared with that using no interlayer. This indicates that the SiO_x interlayer works as an electron-transport and hole-blocking layer. However, J_{sc} and FF are lower with higher R_s than those of other $Ti_mSi_nO_x$-fitted PSCs, which is ascribed to the poorer energy-level alignment with $PC_{71}BM$.

The effects of the optimized $Ti_{0.5}Si_{0.5}O_x$ interlayer on the photovoltaic performance were simply investigated by comparing the $Ti_{0.5}Si_{0.5}O_x$/Al with the three different cathodes: (i) none/Al; (ii) LiF/Al; and (iii) Ca/Al, in a solar cell based on the PBDTTT-F-ECB:$PC_{71}BM$ BHJ (weight ratio 1:2). The thickness (4 nm) of $Ti_{0.5}Si_{0.5}O_x$ was verified from the cross-sectional TEM image of the PSC employing the $Ti_{0.5}Si_{0.5}O_x$ interlayer, as shown in Fig. 3 (a). The presence of Ti and Si in the cathode interlayer was confirmed by EDS spectrum (Fig. 3 (b)) obtained at the point marked with a red open circle in Fig. 3 (a). Fig. 4 (a) and Table 2 show the *J-V* characteristics and efficiency parameters of the four different PSCs, respectively. Notably, J_{sc} of the PSC fitted with

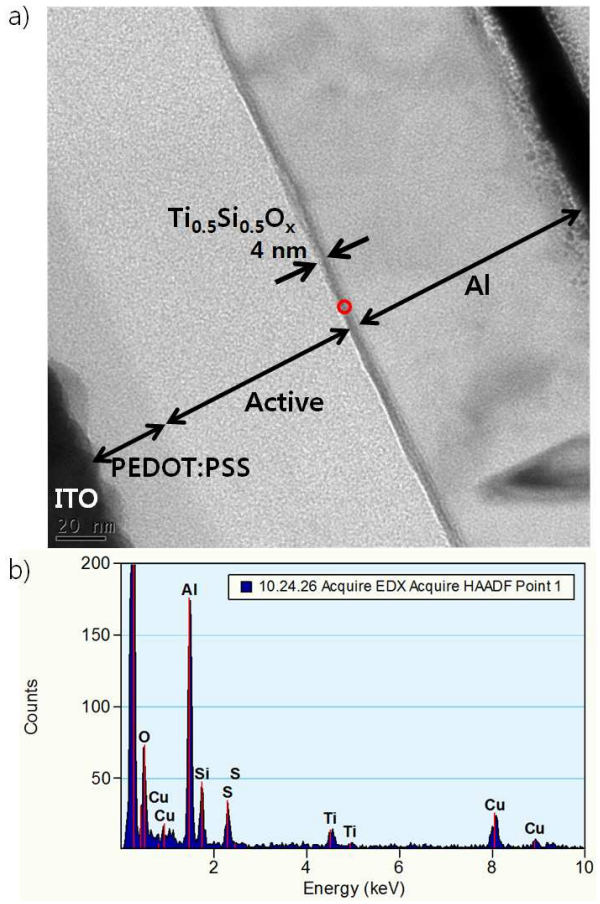

Fig. 3 a) Cross-section TEM image of the device with the $Ti_{0.5}Si_{0.5}O_x$ interlayer. b) EDS spectrum obtained at the red open circle position in the $Ti_mSi_nO_x$ layer in a). Cu peaks are from the Cu TEM grid.

$Ti_{0.5}Si_{0.5}O_x$ is significantly higher than the others, as V_{oc} and FF maintain high values. The incident photon-to-current conversion efficiency (IPCE) of the PSC with $Ti_{0.5}Si_{0.5}O_x$ is higher than the others in the measured wavelength range, except from 400 to 480 nm, where the PSC with no interlayer exhibits higher IPCE (Fig. 4 (b)). This result is consistent with the higher J_{sc} of the PSC with $Ti_{0.5}Si_{0.5}O_x$. The exception might be related with the electric field redistribution or enhancement with the Al-only cathodes in the short wavelength region (400 – 480 nm) but it is not clear yet (see ESI, Fig. S2).

To explain such a high J_{sc} with high IPCE dominating the higher PCE, we measured the total absorption by the active layers of the PSCs. Fig. 4 (c) shows the total absorption in the active layer. The higher absorption of the PSC with $Ti_{0.5}Si_{0.5}O_x$ in most wavelength regions is in good agreement with its higher J_{sc} compared to the PSC with Ca. However, there is no significant difference between the absorption spectra of the PSC with $Ti_{0.5}Si_{0.5}O_x$ and that with no interlayer. A similar absorption spectrum can be expected because of the very thin thickness of the $Ti_{0.5}Si_{0.5}O_x$ layer (~4 nm). A transparent interlayer acting as an optical spacer between the active layer and the reflective Al electrode redistributes the light in the active layer, thus changing the total absorption when the interlayer is sufficiently thick.[5,32,33] The referred results indicate that both thickness and refractive index are critical for the effectiveness of the optical spacer.[34] Considering the two parameters, the $Ti_{0.5}Si_{0.5}O_x$ interlayer is too thin to redistribute the light significantly. This is confirmed by the absorption spectrum obtained from the PSC fitted with LiF.

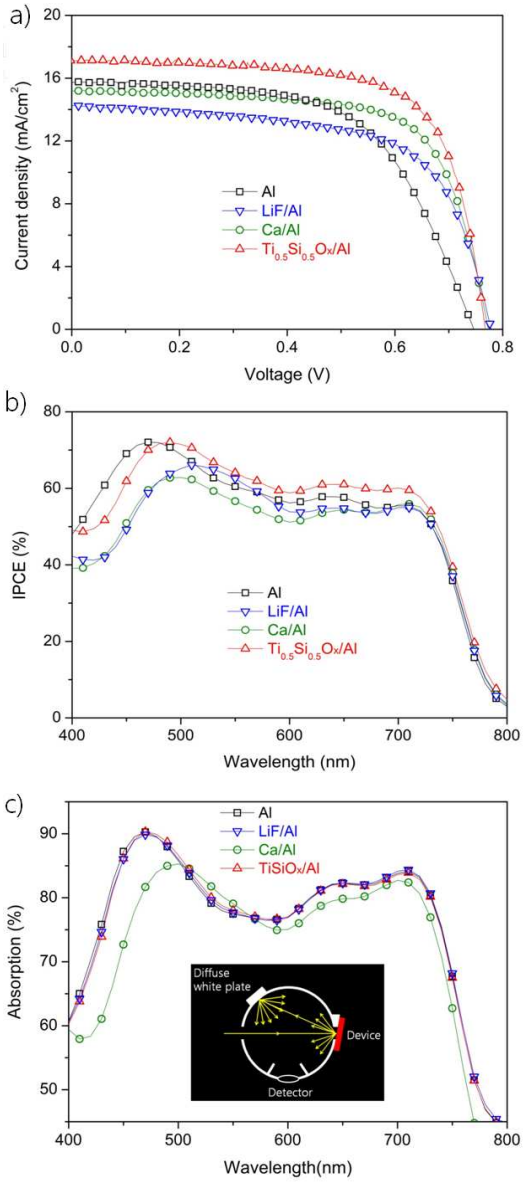

Fig. 4 a) *J-V* characteristics, b) IPCE spectra, and c) total absorption spectra of the PBDTTT-F-ECB:$PC_{71}BM$ BHJ solar cells with the four different cathodes. The inset of c) shows a schematic diagram of an integrating sphere for measuring the total reflection comprising direct and diffuse reflections.

Table 2 Efficiency parameters of the devices employing the four different cathodes.

Interlayer	V_{oc} [mV]	J_{sc} [mA cm^{-2}]	FF [%]	PCE [%]	
				Best	Ave. [a]
None	736	15.0	61.4	6.78	6.72
LiF	776	14.3	64.8	7.19	7.09
Ca	776	14.8	69.2	7.95	7.76
$Ti_{0.5}S_{0.5}O_x$	776	17.2	70.2	9.37	9.25

[a] Average values were obtained from a minimum of 12 devices for each cathode.

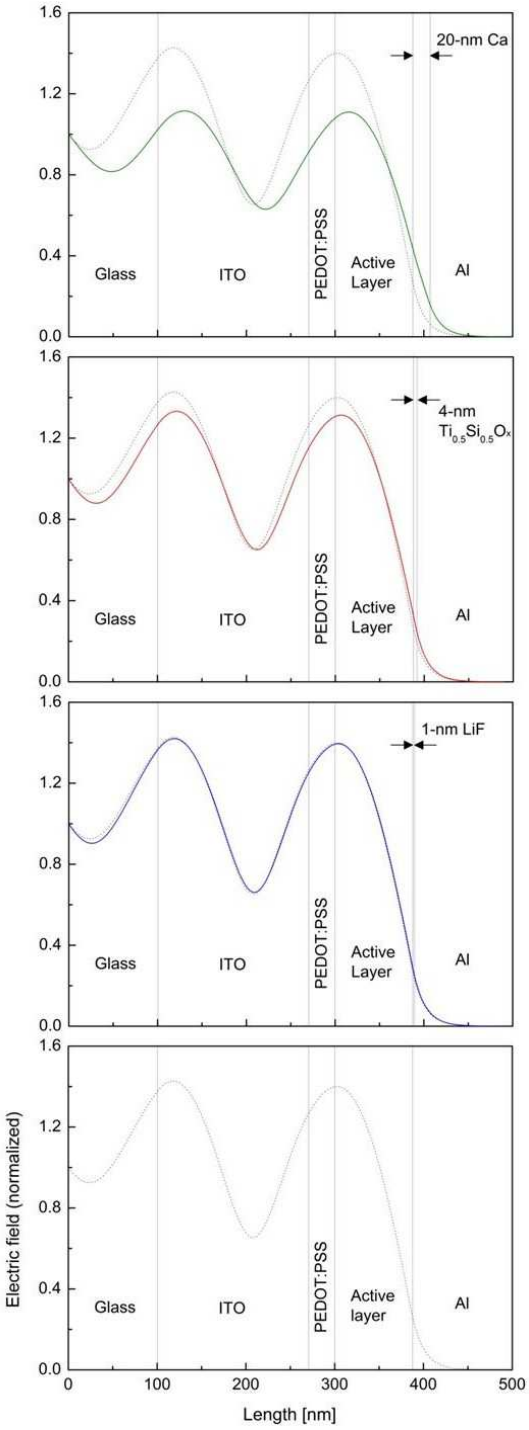

Fig. 5 Calculated electric-field intensity of 650-nm light as a function of position in the solar cells fitted with the four different cathodes. The light grey lines (the electric-field intensity plot for the Al-only cathode which is the same as that of the lowest pannel) are plotted together in the upper three pannels for more convenient comparison).

Because of its thin thickness (1 nm) and similar refractive index (n=1.39, k=0)[35] to that of $Ti_{0.5}Si_{0.5}O_x$ (n=1.54, k=0), the LiF also shows no optical spacer effect. Only the 20-nm thick Ca (n=0.66, k=2.6)[36] layer affects the light redistribution significantly, but the high loss component k reduces the light intensity in the active layer. Light redistribution by each interlayer reconfirms this conclusion. The electric field distribution was calculated with the use of complex indices of refraction and layer thickness.[37] Fig. 5 shows the calculated electric field redistribution of 650-nm light for each interlayer; this is not very marked in the devices with thin or no interlayers, i.e. (i) 1-nm LiF and (ii) 4-nm $Ti_{0.5}Si_{0.5}O_x$, while that in the device with 20-nm Ca is remarkable. We can see that the peak position of the electric field does not change considerably with the LiF nor $Ti_{0.5}Si_{0.5}O_x$ device, while the peak shift is obvious for the device with 20-nm Ca. In addition, because of the high k (2.55), the peak intensity decreases greatly for the device with Ca. This result is consistent with the results of the total absorption measurements. The difference in J_{sc} values between the four PSCs cannot be explained with such similar total light absorptions (except for the Ca device). Therefore, in conclusion, the electron-collection efficiency of each PSC at the cathode should be considered as a key factor (as discussed above) because the cathode interlayer is the sole difference in the device structure.

For verification of the universal effectiveness of the $Ti_{0.5}Si_{0.5}O_x$ interlayer, BHJ solar cells based on $PC_{71}BM$ and three published donor polymers (PTB1,[27] PTB7,[30] and PBDTTT-CF[28]) were additionally tested with three types of cathodes; none/Al, Ca/Al, and $Ti_{0.5}Si_{0.5}O_x$/Al. Improvement in photovoltaic performance induced by the $Ti_{0.5}Si_{0.5}O_x$ interlayer can be also verified for all the additionally tested polymers in spite of their quite different HOMO and LUMO levels. That is because the energy-level alignment needs to be formed only with the LUMO of the acceptor, $PC_{71}BM$, regardless of the donor polymer (The J-V characteristics of the PSCs fabricated with the given three polymers are provided in ESI. (Fig. S3)). Furthermore, since the VBM of $Ti_{0.5}Si_{0.5}O_x$ is much deeper than the HOMO of typical organic donor materials, including the polymers tested in this study, we believe $Ti_{0.5}Si_{0.5}O_x$ will be effective for most organic donor materials in BHJ solar cell applications.

The surface energy of $Ti_mSi_nO_x$ was also changed by adjusting the Si mol% (see ESI, Fig. S4). Surface energy of the cathode interlayer doesn't impact much on the performance of a PSC in a normal architecture used in this work. However, it does significantly when a BHJ layer is formed on the cathode interlayer in an inverted architecture.[24] We believe that this tunable surface energy of $Ti_mSi_nO_x$ may be useful for inverted PSC applications together with its tunable work function.

Conclusions

We have demonstrated enhanced PCE in a PSC fabricated by using a novel method to control the work function of the cathode interlayer to form a cascade energy-level structure from the $PC_{71}BM$ to the cathode. The method utilizes a composition-adjustable ternary oxide, i.e., solution-processed $Ti_mSi_nO_x$. The work function of $Ti_mSi_nO_x$ could be engineered by adjusting the Si mol% during the sol-gel reaction. The bandgap and valence band maxima of $Ti_mSi_nO_x$ were changed simultaneously, enhancing the hole-blocking ability of $Ti_mSi_nO_x$. The PCE enhancement is attributed to the higher electron-collection efficiency due to the well-aligned energy-level structure and better hole-blocking ability caused by the deeper VBM. The $Ti_mSi_nO_x$ sol-gel film is expected to be effective for most organic donor materials; this was verified with a few other published donor polymers.

Acknowledgements

The authors gratefully thank Dr. Dong-Jin Yun for his help with the UPS measurement.

Notes and references

[a] *Samsung Advanced Institute of Technology, Samsung Electronics, Yongin 446-712, South Korea. Fax: +82 31 280 9359; Tel: +82 31 280 9314; E-mail: sg.ihn@samsung.com, yeongsuk.choi@samsung.com*
[b] *School of Chemical Engineering and SKKU Advanced Institute of Nanotechnology, Sungkyunkwan University, Suwon 440-746, South Korea.*

† Electronic Supplementary Information (ESI) available: UV-vis absorbance spectra and surface energies of $Ti_mSi_nO_x$ with various Si mol%, the *J-V* characteristics of the PSCs based on a few published polymers. See DOI: 10.1039/b000000x/

1 G. Yu and A. J. Heeger, *J. Appl. Phys.*, 1995, **78**, 4510.
2 G. Yu, J. Gao, J. C. Hummelen, F. Wudl and A. J. Heeger, *Science*, 1995, **270**, 1789.
3 J. J. M. Halls, C. A. Walsh, N. C. Greenham, E. A. Marseglia, R. H. Friend, S. C. Moratti and A. B. Holmes, *Nature*, 1995, **376**, 498.
4 C. J. Brabec, A. Cravino, D. Meissner, N. S. Sariciftci, T. Fromherz, M. T. Rispens, L. Sanchez, J. C. Hummelen, *Adv. Funct. Mater.* 2001, **11**, 374.
5 J. Y. Kim, S. H. Kim, H.-H. Lee, K. Lee, W. Ma, X. Gong, A. J. Heeger, *Adv. Mater.* 2006, **18**, 572.
6 S. H. Park, A. Roy, S. Beaupré, S. Cho, N. Coates, J. S. Moon, D. Moses, M. Leclerc, K. Lee, A. J. Heeger, *Nature Photon.* 2009, **3**, 297.
7 C. Waldauf, M. Morana, P. Denk, P. Schilinsky, K. Coakley, S. A. Choulis, C. J. Brabec, *Appl. Phys. Lett.* 2006, **89**, 233517.
8 A. Roy, S. H. Park, S. Cowan, M. H. Tong, S. Cho, K. Lee, A. J. Heeger, *Appl. Phys. Lett.* 2009, **95**, 013302.
9 A. Roy, S. H. Park, S. Cowan, M. H. Tong, S. Cho, K. Lee, A. J. Heeger, *Appl. Phys. Lett.* 2009, **95**, 013302.
10 H. Faber, M. Burkhardt, A. Iedaa, D. Kalblein, H. Klauk, M. Halik, *Adv. Mater.* 2009, **21**, 3099.
11 H.-L. Yip, S. K. Hau, N. S. Baek, H. Ma, A. K.-Y. Jen, *Adv. Mater.* 2008, **20**, 2376.
12 S.-G. Ihn, K.-S. Shin, M.-J. Jin, X. Bulliard, S. Yun, Y. S. Choi, Y. Kim, J.-H. Park, M. Sim, M. Kim, K. Cho, T. S. Kim, D. Choi, J.-Y. Choi, W. Choi, S.-W. Kim, *Sol. Energy Mater. Sol. Cells* 2011, **95**, 1610.
13 H. P. Kim, A. R. B. M. Yusoff, J. Jang, *J. Nanosci. & Nanotech.* 2013, **13**, 5142.
14 K.-L. Ou, D. Tadytin, K. X. Steirer, D. Placencia, M. Nguyen, P. Lee, N. R. Armstrong, *J. Mater. Chem. A* 2013, **1**, 6794.
15 Y.-H. Niu, M. S. Liu, J.-W. Ka, A. K.-Y. Jen, *Appl. Phys. Lett.* 2006, **88**, 093505.
16 G. Zhang, W. Li, B. Chu, L. Chen, F. Yan, J. Zhu, Y. Chen, C. S. Lee, *Appl. Phys. Lett.* 2009, **94**, 143302.
17 Y.-J. Cheng, C.-H. Hsieh, Y. He, C.-S. Hsu, Y. Li, *J. Am. Chem. Soc.* 2010**, 132**, 17381.
18 C.-H. Hsieh, Y.-J. Cheng, P.-J. Li, C.-H. Chen, M. Dubosc, R.-M. Liang, C.-S. Hsu, *J. Am. Chem. Soc.* 2010**, 132**, 4887.
19 J. H. Jeon, H. K. Lee, D. H. Wang, S. M. Park, J. W. Kim, K. J. Kim, J. H. Park , O. O. Park, *Sol. Energy Mater. Sol. Cells* 2011, **95**, 2443.
20 F.-L. Kuo, Y. Li, M. Solomon, J. Du, N. D. Shepherd, *J. Phys. D: Appl. Phys.*. 2012, **45**, 065301.
21 S. Bai, Z. Wu, X. Xu, Y. Jin, B. Sun, X. Guo, S. He, X. Wang, Z. Ye, H. Wei, X. Han, W. Ma, *Appl. Phys. Lett.* 2012, **100**, 203906.
22 A. Salomon, D. Berkovich, D. Cahen, *Appl. Phys. Lett.* 2003, **82**, 1051.
23 T. C. Monson, M. T. Lloyd, D. C. Olson, Y. J. Lee, J. W. P. Hsu, *Adv. Mater.* 2008, **20**, 4755.
24 X. Bulliard, S.-G. Ihn, S. Yun, Y. Kim, D. Choi, J.-Y. Choi, M. Kim, M. Sim, J.-H. Park, W. Choi, K. Cho, *Adv. Funct. Mater.* 2010, **20**, 4381.
25 J.-M. Chiu, Y. Tai, *ACS Appl. Mater. Interfaces* 2013, **5**, 6946.
26 M. Song, J.-W. Kang, D.-H. Kim, J.-D. Kwon, S.-G. Park, S. Nam, S. Jo, S. Y. Ryu, C. S. Kim, *Appl. Phys. Lett.* 2013, **102**, 143303.
27 Y. Liang, Y. Wu, D. Feng, S.-T. Tsai, H.-J. Son, G. Li, L. Yu, *J. Am. Chem. Soc.* 2009, **131**, 56.
28 H.-Y. Chen, J. Hou, S. Zhang, Y. Liang, G. Yang, Y. Yang, L. Yu, Y. Wu, G. Li, *Nature Photon.* 2009, **3**, 649.
29 L. Huo, S. Zhang, X. Guo, F. Xu, Y. Li, J. Hou, *Angew. Chem.* 2011, **123**, 9871.
30 Y. Liang, Z. Xu, J. Xia S.-T. Tsai, Y, Wu, G. Li, C. Ray, L. Yu, *Adv. Mater.* 2010, **22**, E135.
31 K. M. Reddya, S. V. Manorama, A. R. Reddy. *Mater. Chem. & Phys.* 2002, **78**, 239.
32 J. Gilot, I. Barbu, M. M. Wienk, R. A. Janssen, *Appl. Phys. Lett.* 2007, **91**, 113520.
33 J. K. Lee, N. E. Coates, S. Cho, N. S. Cho, D. Moses, G. C. Bazan, K. Lee, A. J. Heeger, *Appl. Phys. Lett.* 2008, **92**, 243308.
34 S. B. Jo, J. H. Lee, M. Sim, M. Kim, J. H. Park, Y. S. Choi, Y. Kim, S.-G. Ihn, K. Cho, *Adv. Energy Mater.* 2011, **1**, 690.
35 M. Bass, C. DeCusatis, J. Enoch, V. Lakshminarayanan, G. Li, C. MacDonald, V. Mahajan, E. V. Stryland, *Handbook of Optics Vol. IV: Optical Properties of Materials, Nonlinear Optics, Quantum Optics,* McGraw-Hill, 3rd edn, 2009.
36 C. M. Ramsdale, N. C. Greenham, *J. Phys. D: Appl. Phys.* 2003, **36**, L29.
37 L. A. A. Pettersson , L. S. Roman and O. Inganäs, *J. Appl. Phys.* 1999, **86**, 487.